The Journal of Neuroscience
October 1986, 6(10): 2864-2874

Sprouting of GABAergic Synapses in the Red Nucleus After Lesions of the Nucleus Interpositus in the Cat

Hironobu Katsumaru, Fujio Murakami,* Jang-Yen Wu,† and Nakaakira Tsukahara*,[1]

National Institute for Physiological Sciences, Myodaiji, Okazaki 444, Japan, *Department of Biophysical Engineering, Faculty of Engineering Science, Osaka University, Toyonaka, Osaka 560, Japan, †Department of Physiology, The Milton Hershey Medical Center, The Pennsylvania State University, Hershey, Pennsylvania 17033

An immunocytochemical study using anti-GAD serum was performed to examine the plastic changes of GABAergic inhibitory synapses in the red nucleus (RN) after lesions of the nucleus interpositus (IP) of the cat. Light-microscopic analyses revealed that 20-175 d after the unilateral lesion of the IP, somatic profiles of large neurons in the magnocellular RN contralateral to the lesion were more densely covered with GAD-immunoreactive puncta than those in the ipsilateral RN.

Electron-microscopic analyses demonstrated that the GAD-immunoreactive puncta observed with the light microscope were synaptic terminals and that the number of GAD-immunoreactive synaptic terminals per unit length of somatic membrane of RN neurons was increased on the deafferented side.

The GAD-immunoreactive terminals on somata of RN neurons made symmetric synaptic contacts with somatic membranes on both the deafferented and control sides. The number of immunoreactive synapses on somata of RN neurons was markedly increased on the deafferented side following IP lesion, whereas that of the unlabeled asymmetric synapses was decreased. These observations indicate that new GABAergic synapses were formed on somata of RN neurons after deafferentation from the IP.

Synaptic plasticity in the red nucleus (RN) of the cat has been extensively studied using both physiological and morphological techniques (Fujito et al., 1982; Murakami et al., 1977, 1982; Tsukahara, 1981; Tsukahara et al., 1974, 1975, 1982). One of the remarkable changes is the formation of new corticorubral synapses on the proximal dendrites and somata of the rubrospinal neurons after lesioning the interpositus nucleus (IP) (Murakami et al., 1977, 1982; Tsukahara et al., 1975).

An electrophysiological study demonstrated that stimulation of the corticorubral pathway elicits IPSPs after EPSPs (Tsukahara et al., 1968). In a previous study, we found morphological evidence suggesting that this IPSP is mediated by GABAergic interneurons (Katsumaru et al., 1984). This situation raises the possibility that GABAergic input converging upon RN neurons may be affected by IP lesions as well. Actually, a biochemical study indirectly suggested that plastic changes of the GABAergic input may occur in the RN following cerebellar lesions (Nieoullon and Dusticier, 1981). However, no direct evidence has been presented for the plasticity of GABAergic synapses onto RN neurons.

The present study used immunocytochemical methods to provide morphological evidence for the sprouting of the GABAergic synapses in the RN after lesions of the IP.

Materials and Methods

Animals

Seventeen young cats (0.6–3.0 kg) were used in the present study. Eleven to 175 d before perfusion, the IP of 14 animals was unilaterally ablated by suction with a stereotaxically introduced pipette via a dorsocaudal approach. Completeness of the IP lesion was histologically checked after the experiment. In the remaining 3 animals, lesion of the brain was confined to the overlying cerebellar cortex above the IP for a sham-operated control.

Fixation and immunocytochemistry

Methods of fixation and immunocytochemistry were the same as previously reported (Katsumaru et al., 1984; Murakami et al., 1983). Briefly, cats were deeply anesthetized with sodium pentobarbital (Nembutal) and perfused with a mixture of 4% paraformaldehyde and 0.1% glutaraldehyde in 0.12 M phosphate buffer, pH 7.4. A brain block containing both RNs was carefully dissected with a stereotaxically placed knife and cut into 100-μm-thick frontal sections with a Vibratome. After being incubated in rabbit anti-GAD serum at a dilution of 1:2000 for 17–26 hr at 4°C, the sections were processed for enzyme immunocytochemistry with the peroxidase–antiperoxidase method (Sternberger, 1979) with some modifications (Katsumaru et al., 1984). The anti-GAD serum used in the present study has been well characterized and used extensively for immunocytochemical studies (Wu, 1983; Wu et al., 1982). As a control, nonimmunized rabbit serum was applied instead of the rabbit anti-GAD serum. After reaction with 0.05% diaminobenzidine tetrahydrochloride and 0.01% H_2O_2, the sections were further fixed in 2% osmium tetroxide, stained en bloc with 0.5 or 1.5% uranyl acetate, dehydrated with an ethanol series, and embedded in Quetol 812 (Nissin EM) or Epon 812 (TAAB) between slides and coverslips coated with Teflon (Wilson and Groves, 1979).

Quantitative light-microscopic analysis

The embedded sections were examined under a light microscope. For a quantitative analysis, every neuronal profile more than 30 μm in diameter and possessing a cell nucleus was photographed using Nomarski optics from several sections randomly selected from the caudal magnocellular region of the RN. Since the GAD-immunoreactive reaction product was limited to the superficial portion of the sections (several microns in depth from the surface), samples were taken from the surface of these sections. The perimeter and minor diameter of each soma were measured from the pictures, which were printed at a final magnification of ×600, with an image analyzer (Kontron IBAS 2). GAD-immunoreactive puncta encircling each somatic profile were then traced, and the total area of the puncta was measured from the tracings with the image analyzer.

Received Dec. 6, 1985; revised Apr. 11, 1986; accepted Apr. 11, 1986.

We are grateful to Dr. Toshio Kosaka for his helpful advice; to Drs. Charles Wilson and Richard Penny for critically reading and grammatically improving the manuscript; to Drs. Mitsuo Kawato, Yoichi Oda, and Nobuhiko Yamamoto for valuable discussions. This work was partly supported by Grant-in-Aid for Special Research from the Ministry of Education, Science and Culture, Japan (Project Nos. 59213016 and 59225015).

Correspondence should be addressed to Dr. Fujio Murakami at the above address.

[1] Deceased.

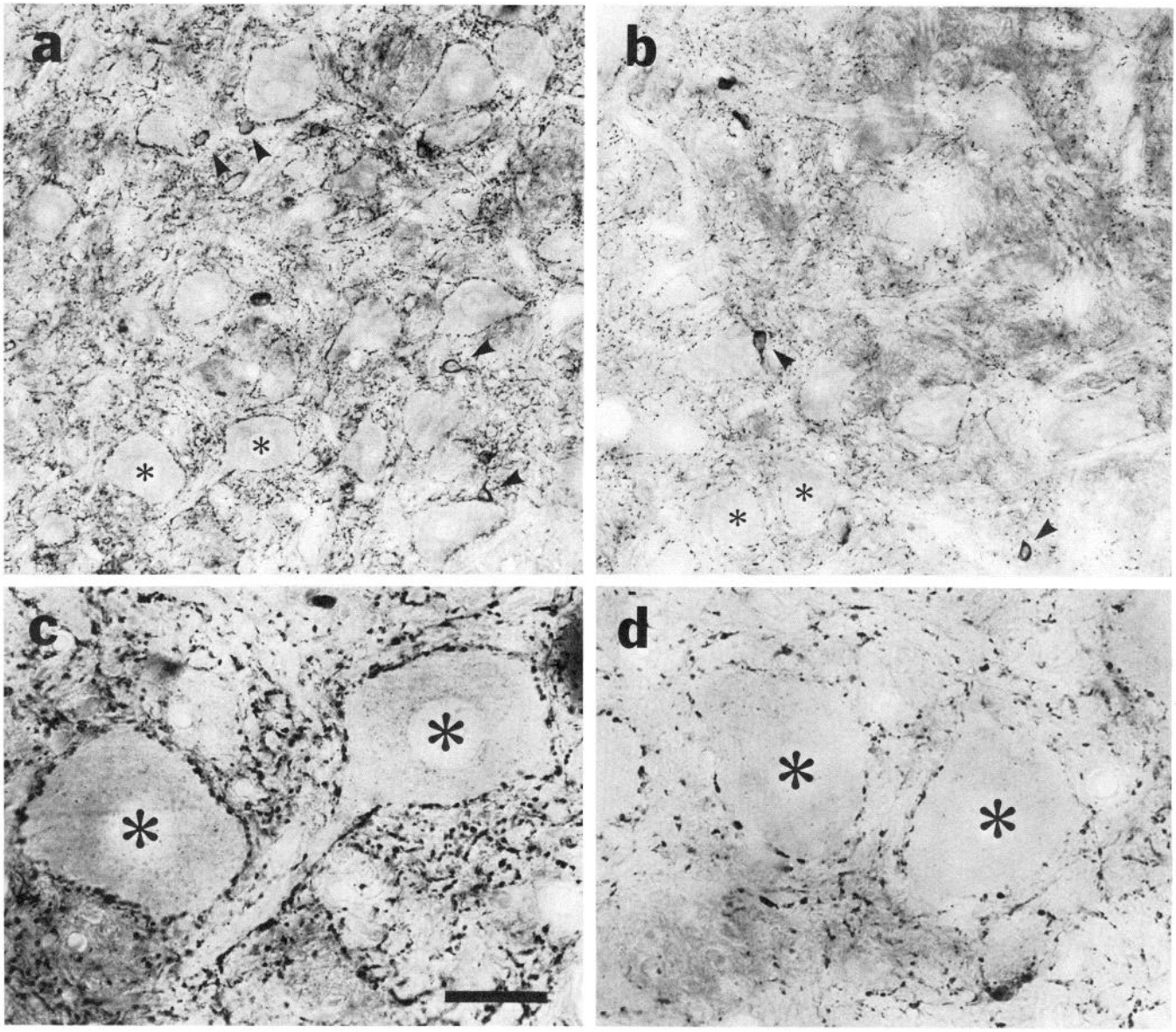

Figure 1. Photomicrographs of a frontal 100-μm-thick section through the RN of an IP-lesioned cat 155 d after operation. *a* and *c*, Deafferented side; *b* and *d*, control side. GAD-immunoreactive reaction product is more densely distributed in the deafferented RN (*a*) than in the control RN (*b*). *Small arrowheads* indicate somata of GAD-immunoreactive neurons. *c* and *d*, High-magnification photomicrographs of the RN neurons marked by asterisks in *a* and *b*, respectively. The magnocellular RN neurons on the deafferented side (*c*) are more densely covered with GAD-immunoreactive puncta than those on the control side (*d*). *a* and *b*, ×180; *c* and *d*, ×500. Bar, 30 μm.

Electron-microscopic analysis

After the light-microscopic examination, some of the embedded sections were cut into thin sections and examined with an EM (Jeol 100-CX) at 80 kV. Electron micrographs of somatic profiles were taken from every few sections and enlarged at a final magnification of ×4600. Montages were made from these electron micrographs, and the number of GAD-immunoreactive terminals attached to somatic membrane of each profile was counted. The perimeter of each somatic profile was measured with an image analyzer (Kontron MOP). The number of GAD-immunoreactive terminals per 100 μm perimeter length of the somatic membrane was then calculated for each somatic profile.

Quantitative electron-microscopic analysis of symmetric and asymmetric synapses

We counted the number of synaptic terminals of symmetric and asymmetric type on RN neurons in an IP-lesioned animal. In this experiment, the method of fixation was partly modified to improve the preservation of the tissue. This animal, whose IP had been lesioned 175 d before, was perfused with a fixative containing 4% paraformaldehyde and 0.4% glutaraldehyde. The fixed brain block was cut alternately into 100- and 200-μm-thick sections. Sections 100 μm thick were processed for GAD immunocytochemistry with the same method as described above, while sections 200 μm thick were fixed with 2% osmium tetroxide immediately after cutting. All the sections were embedded in Epon 812. Sections processed for immunocytochemistry were observed with a light microscope to confirm the increase in immunoreactivity to GAD on the deafferented side. Then thin sections were cut, stained with uranyl acetate and lead citrate, and examined with the EM.

Thin sections cut from Epon blocks without immunocytochemistry were used to classify the types of synapses and count their number. Electron micrographs of somatic profiles of magnocellular RN neurons with cell nucleus were taken along the somatic membrane at a magnification of ×9000. They were printed at a final magnification of ×22,500. Synaptic terminals that were cut at a right angle to synaptic membranes were classified as follows: (1) symmetric synapses displaying symmetric pre- and postsynaptic densities, a synaptic cleft of about 20 nm, and synaptic vesicles accumulated at an active zone; and (2) asymmetric

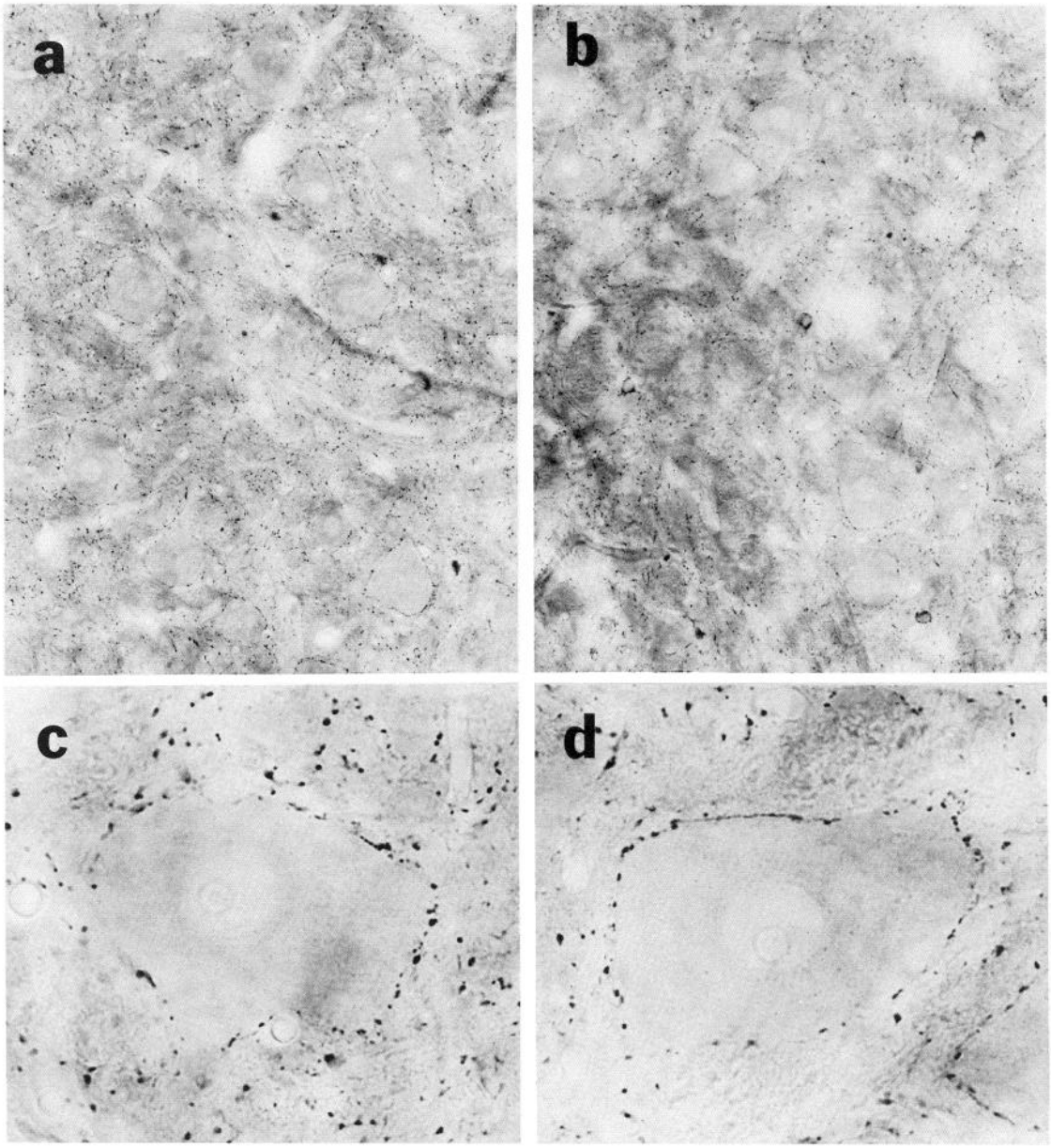

Figure 2. Photomicrographs of the RN of a sham-operated control animal. *a* and *b*, Photomicrographs of the RN on the side contralateral to the lesion (*a*) and on the ipsilateral side (*b*). *c* and *d*, High-magnification photomicrographs of RN neurons in *a* and *b*, respectively. No difference in immunoreactivity between the sides can be seen. *a* and *b*, ×150; *c* and *d*, ×600.

synapses displaying relatively thicker postsynaptic densities, a synaptic cleft of about 30 nm, and synaptic vesicles accumulated at an active zone (Peters et al., 1976).

Thin sections cut from Epon blocks of immunocytochemically stained material were used to clarify the type of GAD-immunoreactive synapses. Electron micrographs of GAD-immunoreactive synaptic terminals on somatic membranes of large RN neurons were taken. GAD-immunoreactive terminals were classified as symmetric or asymmetric synapses according to the criteria described above.

Results

Increased immunoreactivity in deafferented RN

Figure 1, *a* and *b*, shows low-magnification light micrographs of corresponding RN regions from the deafferented and control sides, respectively, in an animal fixed 155 d after the IP lesion. In the RN of the deafferented side (contralateral to the IP lesion), GAD-immunoreactive puncta were more densely distributed than on the control side. The neurons were also more densely packed on the deafferented side (Fig. 1*a*) than on the control side (Fig. 1*b*), probably due to shrinkage of the nucleus.

Another difference between the deafferented and control RN was the density of GAD-immunoreactive puncta encircling each neuronal profile. The neurons marked with asterisks in Figure 1, *a* and *b*, are shown at higher magnification in Figure 1, *c* and *d*, respectively. Neuronal profiles in Figure 1*c* (deafferented side) are more densely covered with GAD-immunoreactive puncta than those in Figure 1*d* (control side). Similar increases in GAD immunoreactivity were observed in 11 other animals whose IP had been lesioned more than 20 d prior to brain perfusion. In 7 of these 12 animals, the lesion of the IP was incomplete; however, the RN of these animals also showed a similar increase in GAD-immunoreactive puncta on the deafferented side.

In control sections treated with normal rabbit serum instead of anti-GAD serum, no reaction product was seen in either RN.

Sham-operated animals

The IP lesions were made by aspiration; the operation also lesions the overlying cerebellar cortex. In order to test the possibility that the lesion of the cerebellar cortex itself might change the GAD immunoreactivity, we made a unilateral lesion of the cerebellar cortex without lesioning the IP in 3 animals.

As shown in Figure 2, *a* and *b*, no difference was observed in the immunoreactivity in the RN of the experimental side (Fig. 2*a*) and that of the control side (Fig. 2*b*) in an animal 70 d after lesioning, nor was there a difference in density of GAD-immunoreactive puncta contacting neuronal profiles (Fig. 2, *c*, *d*). In 2 other animals that underwent sham-operation 41 and 103 d before perfusion, no difference in immunoreactivity between the RN of either side was detected (see Table 1).

Quantitative light-microscopic analysis

In order to quantify the increase in GAD immunoreactivity, we measured the total area of the GAD-immunoreactive puncta encircling each somatic profile of RN neurons. Since the soma perimeter varies from neuron to neuron, we calculated the ratio of the total area of GAD-immunoreactive puncta to the perimeter of each soma to quantify the density of GAD-immunoreactive puncta on each RN neuron. The samples were taken bilaterally from corresponding regions of RN. The data shown in Figure 3 are the result of the measurements from an animal 37 d after an IP lesion. The mean values (±SD) of the ratio for the neurons on the deafferented (*A*) and control (*B*) sides were 0.47 ± 0.20 ($n = 22$) and 0.24 ± 0.10 $\mu m^2/\mu m$ ($n = 22$), respectively. Statistical analysis demonstrated that the mean value for the deafferented side was significantly larger than that for the control side ($p < 0.001$; *t* test). The minor diameter of RN neurons on the deafferented and the control side (Fig. 3) was 40.8 ± 6.0 ($n = 22$) and 42.7 ± 6.4 μm ($n = 22$), respectively. There was no statistically significant difference in the minor diameter between neurons sampled from the RN on either side. Quantitative analysis was performed in 2 other IP-lesioned animals with similar results.

Ultrastructural correlate for GAD-immunoreactive puncta

The GAD-immunoreactive puncta observed under the light microscope looked like synaptic terminals. To check this, we examined the same GAD-immunoreactive puncta contacting an RN neuron with both light and electron microscopes. Figure 4*a* shows a light micrograph of an RN neuron on the deafferented side. The Epon block containing that neuron was cut into thin sections and examined with the EM. An electron micrograph of the corresponding region (boxed area in Fig. 4*a*) is shown in Figure 4*b*. All the GAD-immunoreactive puncta surrounding the soma under the light microscope corresponded to GAD-immunoreactive boutons in the electron micrograph (Fig. 4, *a*, *b*). Some of the GAD-immunoreactive terminals made synaptic contact with the soma in the plane of the section (Fig. 4*c*). Although most of the GAD-immunoreactive puncta looked like synaptic endings with synaptic vesicles, some of them in the neuropil of the RN looked like dendritic profiles.

By making semiserial sections, it was possible to identify the individual GAD-immunoreactive boutons, some of which appeared to be strings of GAD-immunoreactive puncta with a light microscope. Figure 4*d* shows a drawing of GAD-immunoreactive boutons made from montages of electron micrographs of semiserial sections. Each dot in Figure 4*d* therefore represents identified individual GAD-immunoreactive boutons.

Comparison of Figure 4*a* with 4*b* shows that the GAD-immunoreactive puncta observed with a light microscope correspond to boutons closely attached to the soma. It is very likely that most of these boutons make synaptic contact with the RN neuron.

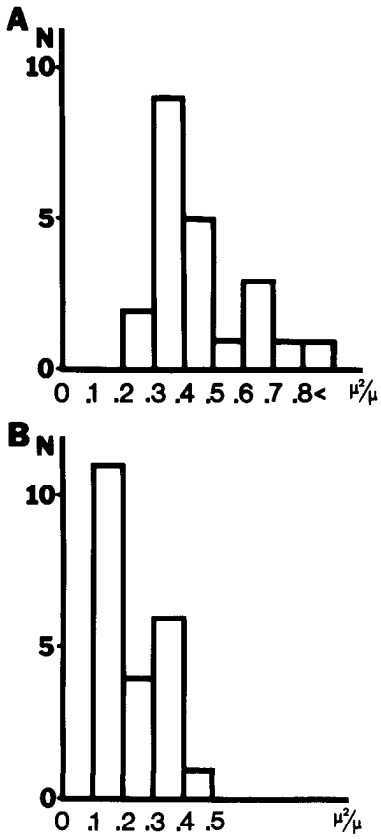

Figure 3. Distribution histograms of the ratio of the total area of the GAD-immunoreactive puncta surrounding the soma to the perimeter of the soma. *A*, Deafferented side; *B*, control side ($n = 22$ for each). *Ordinate*, Number of RN neurons. The values were obtained from an animal 37 d after IP lesioning. The mean value (±SD) for the deafferented side (0.47 ± 0.20 $\mu m^2/\mu m$) was significantly larger than that for the control side (0.24 ± 0.10 $\mu m^2/\mu m$) ($p < 0.001$; *t* test).

Increase in the density of GAD-immunoreactive boutons

In order to determine the ultrastructural correlates of the increased number of GAD-immunoreactive puncta, we compared the ultrastructure of the RN neurons on the deafferented side with that on the control side. Figure 5, *a* and *b*, shows light micrographs of RN neurons surrounded by GAD-immunoreactive puncta on the deafferented side and the control side, respectively. The neuron shown in Figure 5*a* is evidently more densely surrounded with GAD-immunoreactive puncta than the one in 5*b*. Figure 5, *c* and *d*, shows drawings traced from montages of electron micrographs corresponding to the light micrographs of Figure 5, *a* and *b*, respectively.

Figure 5, *e* and *f*, shows drawings made by the same method as those in Figure 4*d*. The number of GAD-immunoreactive terminals per 100 μm somatic perimeter in the deafferented and the control side was 33.1 and 14.9, respectively. These results indicate that the increase in the density of GAD-immunoreactive puncta observed with the light microscope corresponds to an increase in the number of GAD-immunoreactive boutons, presumably synaptic terminals.

The size of GAD-immunoreactive boutons did not seem to differ in the RN of either hemisphere.

Persistent increase in immunoreactivity

The apparent increase in the number of GAD-immunoreactive terminals could be due to an increase in the level of GAD within the preexisting terminals and/or to morphological change, i.e., the proliferation of GABAergic terminals by collateral sprout-

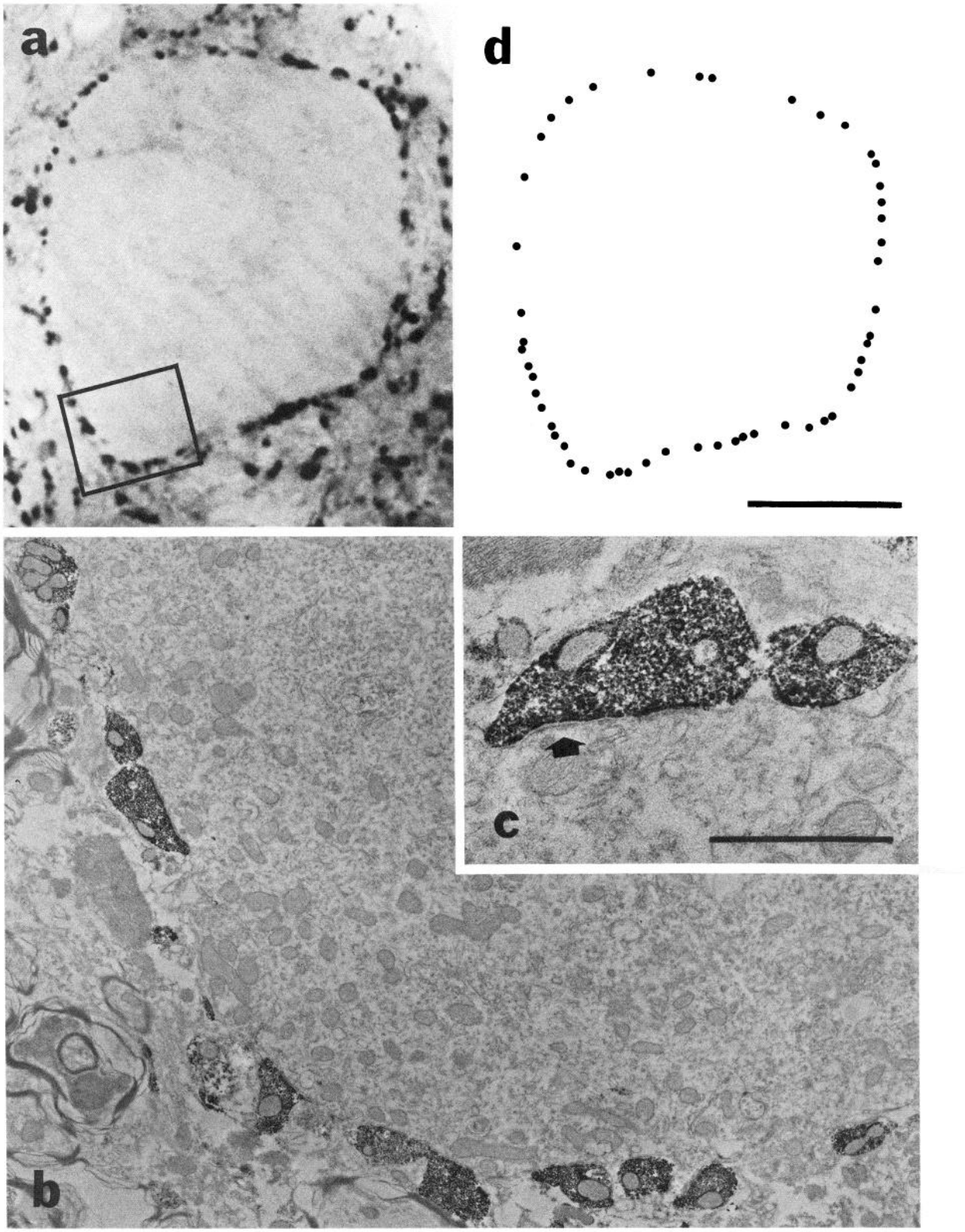

Figure 4. Light and electron micrographs of GAD-immunoreactive puncta surrounding the soma of an RN neuron on the deafferented side and a drawing demonstrating individual GAD-immunoreactive boutons on the soma. *a,* Light micrograph of an RN neuron on the deafferented side. *b,* Electron micrograph of the region enclosed by the *open block* in *a.* Each GAD-immunoreactive bouton corresponds to GAD-immunoreactive puncta in the light micrograph. *c,* Electron micrograph at higher magnification of synaptic terminals shown in *b.* The *arrow* indicates a synaptic specialization (not counterstained). *d,* Drawing made from montages of electron micrographs of semiserial sections. GAD-immunoreactive boutons were traced from each montage, and all the boutons obtained from different sections were superimposed on a single plane. Individual synaptic terminals are shown by *dots. a* and *d,* ×1300 (bar, 20 μm); *b,* ×11,700; *c,* ×31,500 (bar, 1 μm).

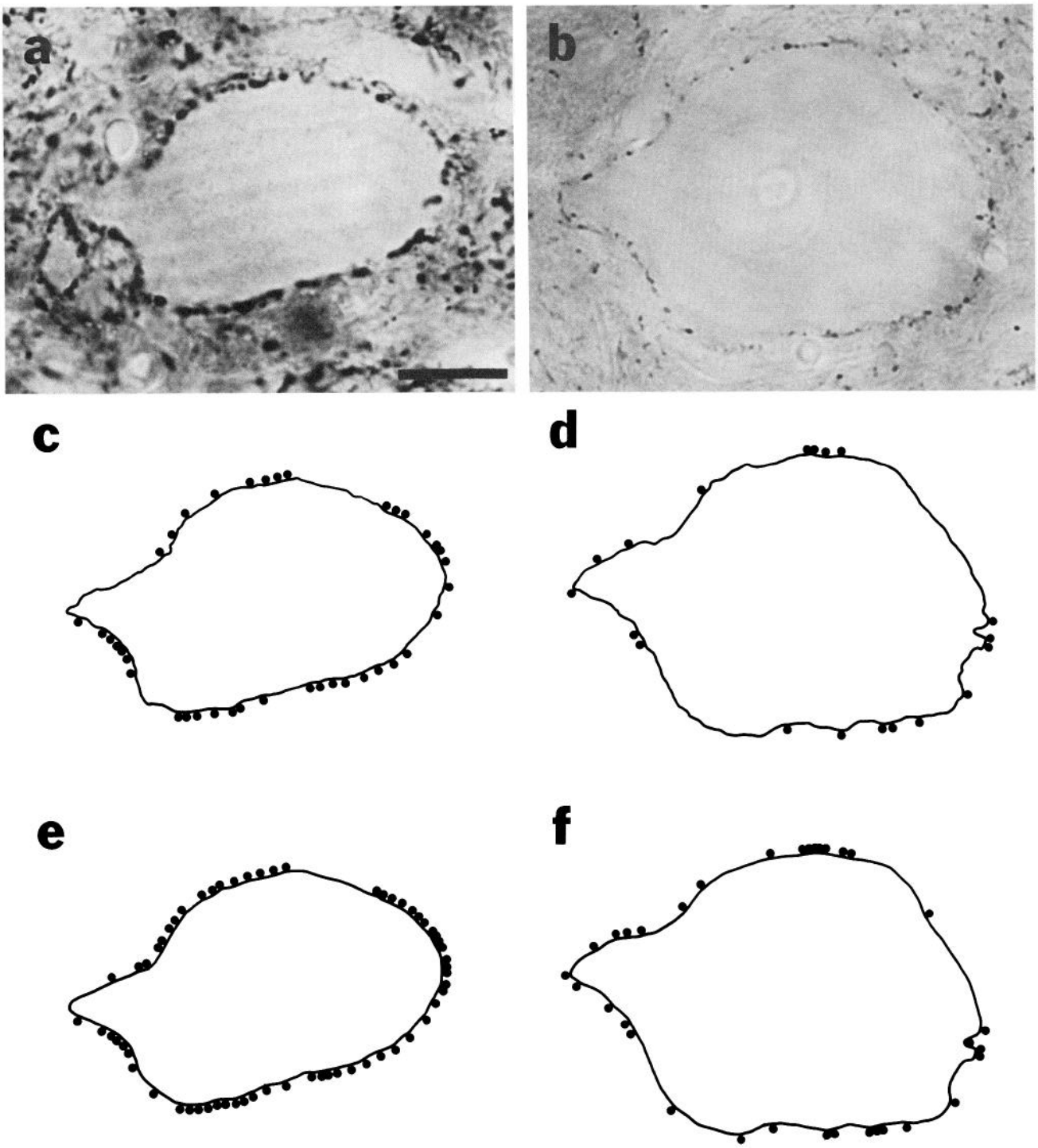

Figure 5. Photomicrographs and drawings of GAD-immunoreactive puncta surrounding somata of RN neurons. *a, c,* and *e,* Deafferented side; *b, d,* and *f,* control side. *a* and *b,* Light micrographs of RN neurons. *c* and *d,* Traces from montages of electron micrographs of a single thin section of the same neurons as shown in *a* and *b,* respectively. Each GAD-immunoreactive synaptic terminal that attaches to the somatic membrane is represented by a *dot*. *e* and *f,* Traces made by the same method as used in Figure 4*d*. The density of GAD-immunoreactive terminals on the deafferented side, judged from both single and reconstructed traces, is larger than that on the control side. ×900. Bar, 20 μm.

ing. It is important to know the time course of the changes in GAD immunoreactivity, because some biochemical changes after deafferentation are transient and do not persist for long (Gilad and Reis, 1979a, b).

In order to determine the time course of the changes in GAD immunoreactivity in our preparation, we examined the animals at various periods after the IP was lesioned. In a cat lesioned 11 d before perfusion, no change in the density of GAD-immunoreactive puncta on RN neurons was noted. In an animal lesioned 15 d before perfusion, there was a slight increase in immunoreactivity in some RN neurons, but most of the GAD-immunoreactive puncta remained unchanged (Fig. 6, *a, b*). Significant changes were first observed in a cat with a survival period of 20 d (Fig. 6, *c, d*). The results obtained from 17 animals

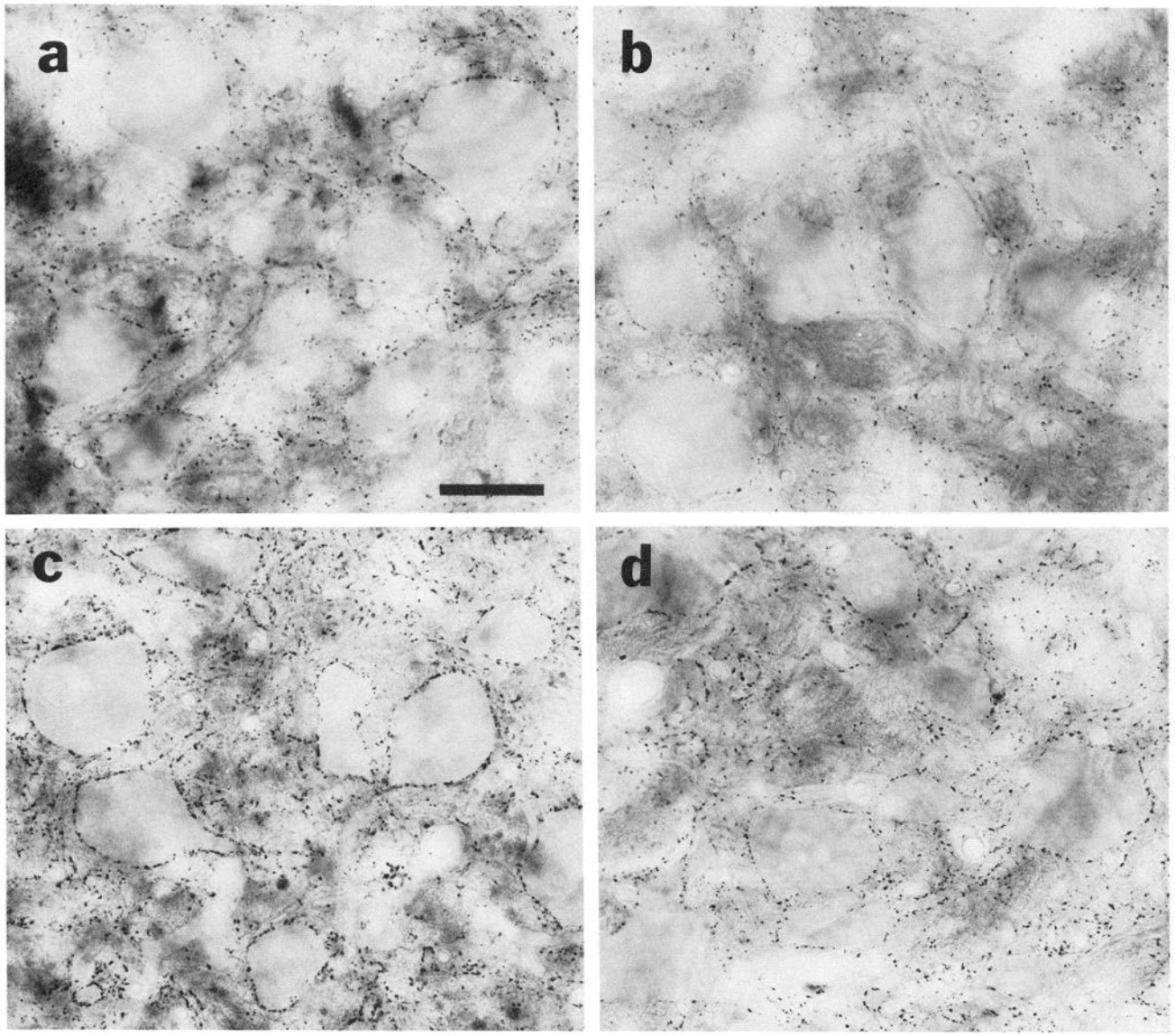

Figure 6. Photomicrographs of the RN in animals with short survival periods after IP lesioning. *a* and *b,* RN neurons in the cat after 15 d. Some of the RN neurons on the deafferented side (*a*) are more densely covered with GAD-immunoreactive puncta than the RN neurons on the control side (*b*). However, the puncta on most of the RN neurons remained unchanged. *c* and *d,* RN neurons in a cat after 20 d. The RN neurons on the deafferented side (*c*) are more densely covered with GAD-immunoreactive puncta than those on the control side (*d*). ×300. Bar, 50 μm.

with various survival periods are summarized in Table 1. The increase in the density of GAD-immunoreactive puncta, first observed at 20 d after operation, persisted for about 6 months.

GAD-immunoreactive terminals form symmetric synapses

The persistent increase in the number of GAD-immunoreactive puncta suggests that this change is due to proliferation of GABAergic terminals rather than to a change in the level of GAD within preexisting terminals. To confirm this hypothesis we examined the change in the number of symmetric terminals synapsing on the RN neurons. GABAergic terminals have been demonstrated to form symmetric synapses in various loci in the CNS (Hendrickson et al., 1983; Hendry et al., 1983; Houser et al., 1983; Ribak et al., 1981; Wood et al., 1976). If this is true in the RN, and if GABAergic terminals proliferate, we might find an increase in the number of symmetric synapses in the deafferented RN.

As exemplified in Figure 7, all the observed GAD-immunoreactive terminals made symmetric synaptic contacts with somata of RN neurons on both the deafferented and control sides. The GAD-immunoreactive synaptic terminal shown in Figure 7*b* exhibits characteristic features of symmetric synapses. It shows symmetric pre- and postsynaptic densities and flattened (or pleomorphic) synaptic vesicles concentrated at the active zone (Peters et al., 1976).

Increase in the number of symmetric synapses

Next, we examined the number of synaptic terminals making symmetric and asymmetric contacts with the somata of RN neurons. Brain sections without immunocytochemical labeling were used in this analysis. We first confirmed that the GAD immunoreactivity was increased on the deafferented side. For this we used neighboring sections processed for immunocytochemistry in the same animal (see Materials and Methods). We then analyzed axosomatic synapses observed in the sections from the same animal but treated to optimize preservation of synaptic morphology. Terminals that formed synaptic contacts in the plane of section were classified as symmetric or asym-

Table 1. Summary of changes in GAD-immunoreactive puncta on RN neurons in cats with IP lesions and sham operations

Post-operative day	IP lesion	Sham operation
11	−	
15	±	
20	+[a]	
30	+[a]	
37	+	
39	+	
41		−
44	+	
70		−
97	+	
103		−
147	+	
155	+	
172	+	
175	+	

Symbols: +, RN neurons in the deafferented side were more densely covered with GAD-immunoreactive puncta; ±, increased immunoreactivity in the deafferented side was observed in some of RN neurons; −, no change was observed.
[a] Two cats.

metric synapses, and the number of symmetric and asymmetric synapses per 100 μm somatic perimeter of RN neurons was counted. Examples of the synaptic terminals observed on RN somata in this material are shown in Figure 8. Synapses corresponding to those stained using GAD immunocytochemistry with flattened (or pleomorphic) vesicles and symmetric synaptic specializations (Fig. 8*a*) are clearly distinguishable from terminals corresponding to the unlabeled type, which have round vesicles and asymmetric specializations (Fig. 8*b*).

The results of the measurements from 40 RN neurons taken from the deafferented and the control sides are shown in Figure 9. The number of symmetric synapses per 100 μm for the neurons on the deafferented (*A*) and the control (*B*) sides was 4.41 ± 1.27 and 2.09 ± 1.48 (mean ± SD, $n = 20$), respectively (Fig. 9, *A, B*). This value for the deafferented side is significantly larger than that for the control side ($p < 0.001$; t test), indicating that the number of symmetric synaptic terminals on the RN neurons was significantly increased after IP lesions. In contrast to symmetric synapses, asymmetric synapses on the deafferented side were significantly decreased following IP lesions (Fig. 9, *C, D*), probably due to loss of interpositorubral synapses.

Discussion

The results presented above support the view that new GABAergic synapses were formed on the somata of the RN neurons following IP lesions.

Immunocytochemical method

The intensity of immunocytochemical reaction varies among sections and animals. It also depends on the method of fixation and the immunocytochemical procedure. However, in the present study, we compared immunoreactivity in the RN of the deafferented side with that of the control side in the same section. This means that the RN on both sides were processed under the same conditions throughout the experiment. Therefore, it is unlikely that the changes observed in the present study are due to variations of immunocytochemical staining.

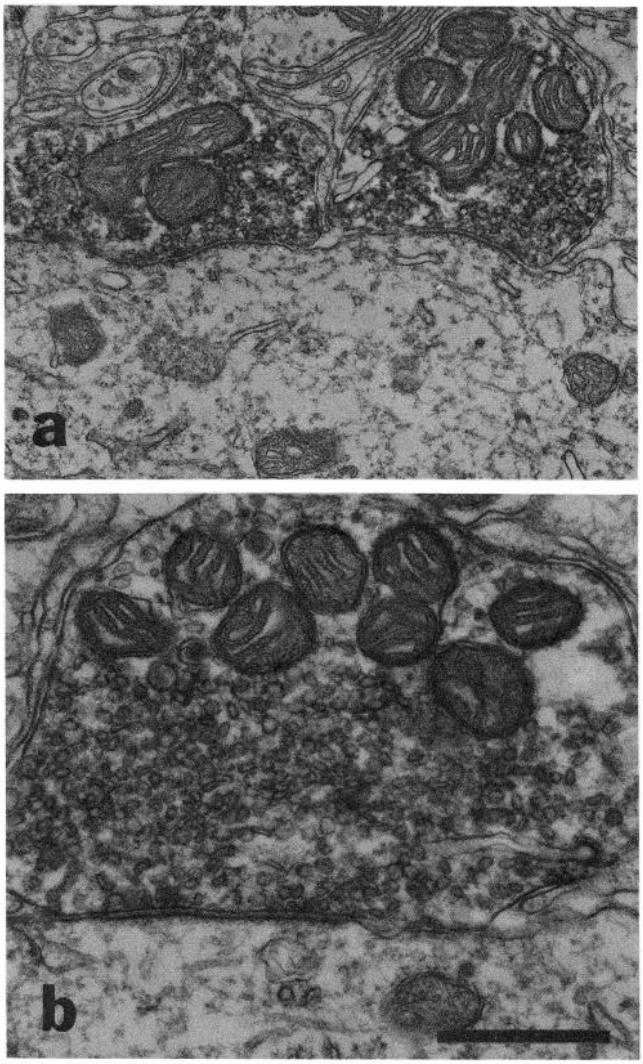

Figure 7. GAD-immunoreactive terminals synapsing on somata of RN neurons on the deafferented side in an animal 175 d after IP lesioning. *a*, GAD-immunoreactive terminals closely located on the somatic membrane. *b*, High-magnification electron micrograph of GAD-immunoreactive terminal. Symmetric synaptic junctions and pleomorphic vesicles are clearly seen seen. *a*, × 27,000; *b*, ×45,000. Bar, 0.5 μm.

Tissue shrinkage

The observed increase in the overall density of GAD-immunoreactive puncta may partly be explained by tissue shrinkage as well as by the increase in the density of GAD-immunoreactive puncta on RN neurons, and, in fact, the RN on the deafferented side was smaller. However, we compared the density of GAD-immunoreactive puncta surrounding RN neurons, and this parameter was not affected by the shrinkage of the nucleus.

The difference in this parameter between the RN of the deafferented and control sides might be caused by the shrinkage of individual RN neurons. However, in the quantitative light-microscopic analysis, we sampled every neuronal profile whose diameter was greater than 30 μm (see Materials and Methods in detail) and found that there were similar numbers of RN neurons of this size on each side (e.g., $n = 22$ for each side in Fig. 3). In addition, there was no statistically significant difference in the minor diameter of RN neurons between the deafferented and the control side (see Results). Therefore, it is unlikely that the increase in the density of the GAD-

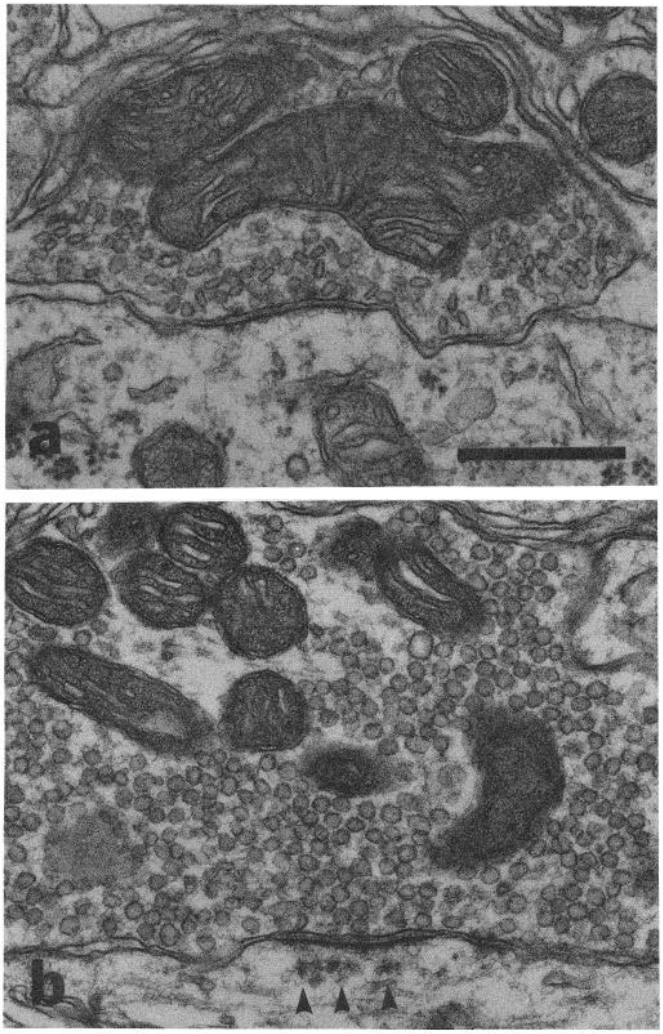

Figure 8. Electron micrographs of terminals synapsing on somatic profile of RN neurons in the same animal as in Figure 7. *a,* Synaptic terminal making symmetric contact with soma on the deafferented side. This terminal exhibits symmetric pre- and postsynaptic densities and has flattened synaptic vesicles. *b,* Synaptic terminal making asymmetric contact with a soma on the deafferented side. This terminal exhibits relatively thicker postsynaptic densities and round synaptic vesicles accumulated at the active zone. A dense body is seen beneath the postsynaptic density (*arrowheads*). ×45,000. Bar, 0.5 μm.

immunoreactive puncta encircling the somata of RN neurons was due to the shrinkage of the tissue.

Sham-operated control

In the present study we aspirated the IP with a pipette via a dorsocaudal approach. This procedure also lesioned the overlying cerebellar cortex. The changes in immunoreactivity might have been solely due to the lesion of the cerebellar cortex. However, no change in immunoreactivity was observed in the RN of 3 sham-operated control animals in which a lesion of the cerebellar cortex was made without lesioning the IP. Therefore, it is unlikely that the changes in GAD-immunoreactivity were due to the lesioning of the cerebellar cortex.

Increase in the number of GABAergic terminals is due to proliferation of the terminals

We demonstrated (1) that the number of GAD-immunoreactive synaptic terminals was increased, (2) that the number of symmetric synapses was increased in the RN of the deafferented

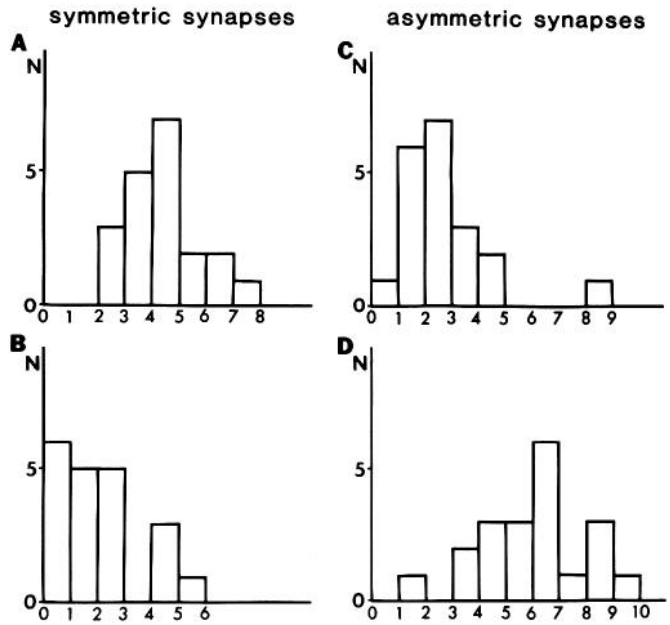

Figure 9. Distribution histograms of the density of symmetric and asymmetric terminals synapsing on somatic profiles. *Abscissa,* Number of synaptic terminals per 100 μm of somatic perimeter ($n = 20$ on each side). *Ordinate,* Number of RN neurons. *A* and *B,* Symmetric synapses. The mean value (±SD) of symmetric synaptic terminals on the deafferented side (*A,* 4.41 ± 1.27) was significantly larger than that on the control side (*B,* 2.09 ± 1.48) ($p < 0.001$, *t* test). *C* and *D,* Asymmetric synapses on the deafferented and the control sides, respectively. See text for further explanation.

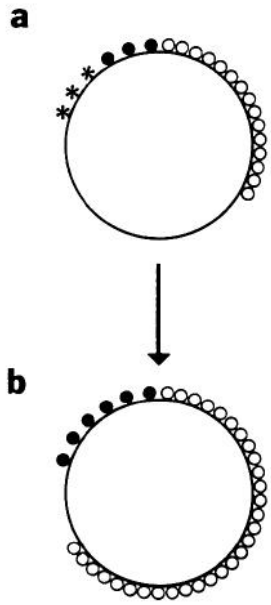

Figure 10. Schematic drawing illustrating the apparent increase in the number of GAD-immunoreactive terminals and symmetric synapses without terminal proliferation of GABAergic synapses. *Small circles* and *asterisks* (○, ●, ∗) represent symmetric terminals on somata of RN neurons (*large circles*). Symbols: ○, non-GABAergic terminal; ●, GABAergic and immunoreactive terminal; ∗, GABAergic but nonimmunoreactive terminal. These are GAD-negative because of an insufficient level of GAD. The number of non-GABAergic but symmetric synaptic terminals (○) is doubled but that of GABAergic terminals (● and ∗) does not change after IP lesioning. The number of GAD-immunoreactive terminals, however, is doubled because the level of GAD is increased and initially GAD-negative terminals (∗) become GAD-positive.

side, and (3) that GAD-immunoreactive terminals form symmetric synapses. All of these observations are consistent with the view that new GABAergic synapses were formed after deafferentation.

However, an alternative mechanism could also explain the increased number of GAD-immunoreactive puncta, i.e., an increase in the level of GAD in preexisting terminals. The three results listed above can be explained if (a) most of the symmetric synapses surrounding the soma of RN are non-GABAergic, and (b) the number of symmetric but non-GABAergic synapses increased in parallel with the increase in the level of GAD within preexisting GABAergic terminals. In fact, many symmetric but nonimmunoreactive synapses were observed in the RN, although it is impossible to determine whether they were genuinely non-GABAergic or were false-negatives caused by insufficient penetration of the antiserum.

The data shown in Figure 3 indicate that the number of GAD-immunoreactive synapses on the deafferented side was about twice that of the control side, assuming that the size of each terminal was the same. This difference fully explains the difference in the number of symmetric synapses shown in Figures 9, *A* and *B*. This quantitative coincidence of the data shown in Figures 3 and 9, *A* and *B*, could still be explained without assuming a proliferation of GABAergic terminals, if most of the symmetric synapses on the somata of RN neurons were non-GABAergic, and if the ratio of the increase of GAD-immunoreactive terminals and symmetric terminals were the same. In Figure 10*a*, we consider an RN neuron surrounded by a large number of non-GABAergic terminals but with symmetric synapses and many fewer GABAergic terminals in the normal condition. Since we assume that the numbers of both non-GABAergic terminals (N_a) and of GAD-immunoreactive terminals doubled after the IP lesion (Fig. 10*b*), the total number of symmetric synapses after IP lesion (T') would be about twice that before lesioning (T), even if the number of GABAergic terminals (N_b) were unchanged, i.e., $T' \approx 2T$, since $T = N_a + N_b$ and $T' = 2N_a + N_b$; $N_a \gg N_b$. It would then be expected that a large proportion of the somatic membrane of RN neurons would be surrounded with non-GABAergic terminals with symmetric synapses after deafferentation (see Fig. 10*b*).

However, as can be seen in the electron micrograph in Figure 4 and the light micrographs in Figures 1, 4, 5, and 6, the somatic membrane of RN neurons was densely surrounded with GAD-immunoreactive terminals on the side of deafferentation. The actual density of GABAergic terminals may be even larger, since some may be nonimmunoreactive as a result of insufficient penetration of antiserum. This quantitative inconsistency derives from the assumption that most of the symmetric synapses are non-GABAergic. Therefore, the most likely explanation for the increase in the number of GABAergic synapses on the somatic membranes of RN neurons is proliferation of GABAergic terminals. The fact that the increase in immunoreactivity for GAD persisted up to 175 d also suggests that this change is accompanied by some morphological change.

Nakamura et al. (1978) showed that the density of axosomatic terminals with pleomorphic and/or flattened vesicles (F-terminals) was increased 11–63 d after IP lesions. Since GABAergic terminals forming symmetric synapses with somata of RN neurons contain flattened or pleomorphic vesicles, their results may also indicate that new GABAergic synapses are formed on the RN neurons after IP lesioning.

Origin of GABAergic terminals

In previous studies, we reported that GABAergic terminals synapse on rubrospinal neurons (Murakami et al., 1983) and that the major source of these terminals is represented by GABAergic intrinsic interneurons that receive input from the sensorimotor cortex (Katsumaru et al., 1984). The GAD-immunoreactive terminals that increased in number following deafferentation may also be synaptic terminals of intrinsic interneurons, although it is possible that some of them were of extrinsic origin.

In conclusion, the findings of the present study can be explained in a consistent way by the view that the proliferation of GABAergic synapses on the somata of RN neurons occurred as a result of collateral sprouting from intrinsic interneurons following deafferentation from the IP.

References

Fujito, Y., N. Tsukahara, Y. Oda, and M. Yoshida (1982) Formation of functional synapses in the adult cat red nucleus from the cerebrum following cross-innervation of forelimb flexor and extensor nerves. II. Analysis of newly appeared synaptic potentials. Exp. Brain Res. *45:* 13–18.

Gilad, G. M., and D. J. Reis (1979a) Transneuronal effects of olfactory bulb removal on choline acetyltransferase and glutamic acid decarboxylase activities in the olfactory tubercle. Brain Res. *178:* 185–190.

Gilad, G. M., and D. J. Reis (1979b) Collateral sprouting in central mesolimbic dopamine neurons: Biochemical and immunocytochemical evidence of changes in the activity and distribution of tyrosine hydroxylase in terminal fields and in cell bodies of A10 neurons. Brain Res. *160:* 17–36.

Hendrickson, A. E., M. P. Ogren, J. E. Vaughn, R. P. Barber, and J.-Y. Wu (1983) Light and electron microscopic immunocytochemical localization of glutamic acid decarboxylase in monkey geniculate complex: Evidence for GABAergic neurons and synapses. J. Neurosci. *3:* 1245–1262.

Hendry, S. H. C., C. R. Houser, E. G. Jones, and J. E. Vaughn (1983) Synaptic organization of immunocytochemically identified GABA neurons in the monkey sensory-motor cortex. J. Neurocytol. *12:* 639–660.

Houser, C. R., M. Lee, and J. E. Vaughn (1983) Immunocytochemical localization of glutamic acid decarboxylase in normal and deafferented superior colliculus: Evidence for reorganization of γ-aminobutyric acid synapses. J. Neurosci. *3*: 2030–2042.

Katsumaru, H., F. Murakami, J.-Y. Wu, and N. Tsukahara (1984) GABAergic intrinsic interneurons in the red nucleus of the cat demonstrated with combined immunocytochemistry and anterograde degeneration methods. Neurosci. Res. *1:* 35–44.

Murakami, F., N. Tsukahara, and Y. Fujito (1977) Analysis of unitary EPSPs mediated by the newly-formed cortico-rubral synapses after lesion of the nucleus interpositus of the cerebellum. Exp. Brain Res. *30:* 233–243.

Murakami, F., H. Katsumaru, K. Saito, and N. Tsukahara (1982) A quantitative study of synaptic reorganization in red nucleus after lesion of the nucleus interpositus of the cat: An electron microscopic study involving intracellular injection of horseradish peroxidase. Brain Res. *242:* 41–53.

Murakami, F., H. Katsumaru, J.-Y. Wu, T. Matsuda, and N. Tsukahara (1983) Immunocytochemical demonstration of GABAergic synapses on identified rubrospinal neurons. Brain Res. *267:* 357–360.

Nakamura, Y., N. Mizuno, and A. Konishi (1978) A quantitative electron microscope study of cerebellar axon terminals on the magnocellular red nucleus neurons in the cat. Brain Res. *147:* 17–27.

Nieoullon, A., and N. Dusticier (1981) Increased glutamate decarboxylase activity in the red nucleus of the adult cat after cerebellar lesions. Brain Res. *224:* 129–139.

Peters, A., S. Palay, and H. de F. Webster (1976) *The Fine Structure of the Nervous System: The Neurons and Supporting Cells,* Saunders, Philadelphia, PA.

Ribak, C. E., J. E. Vaughn, and R. P. Barber (1981) Immunocytochemical localization of GABAergic neurones at the electron microscopical level. Histochem. J. *13:* 555–582.

Sternberger, L. A. (1979) *Immunocytochemistry,* 2nd ed., pp. 104–169, Wiley, New York.

Tsukahara, N. (1981) Sprouting and the neuronal basis of learning. Trends Neurosci. *4:* 1–4.

Tsukahara, N., D. R. G. Fuller, and V. B. Brooks (1968) Collateral pyramidal influences on the corticorubrospinal system. J. Neurophysiol. *31:* 467–484.

Tsukahara, N., H. Hultborn, and F. Murakami (1974) Sprouting of cortico-rubral synapses in red nucleus neurones after destruction of the nucleus interpositus of the cerebellum. Experientia *30:* 57–58.

Tsukahara, N., H. Hultborn, F. Murakami, and Y. Fujito (1975) Electrophysiological study of formation of new synapses and collateral sprouting in red nucleus neurons after partial denervation. J. Neurophysiol. *38:* 1359–1372.

Tsukahara, N., Y. Fujito, Y. Oda, and J. Maeda (1982) Formation of functional synapses in the adult cat red nucleus from the cerebrum following cross-innervation of forelimb flexor and extensor nerves. I. Appearance of new synaptic potentials. Exp. Brain Res. *45:* 1–12.

Wilson, C. J., and P. M. Groves (1979) A simple and rapid section embedding technique for sequential light and electron microscopic examination of individually stained central neurons. J. Neurosci. Methods *1:* 383–391.

Wood, J. G., B. J. McLaughlin, and J. E. Vaughn (1976) Immunocytochemical localization of GAD in electron microscopic preparations of rodent CNS. In *GABA in Nervous System Function,* E. Roberts, T. N. Chase, and D. B. Tower, eds., pp. 133–148, Raven Press, New York.

Wu, J.-Y. (1983) Preparation of glutamic acid decarboxylase as immunogen for immunocytochemistry. In *Neuroimmunocytochemistry* (IBRO Handbook Series: Methods in the Neurosciences), A. C. Cuello, ed., pp. 159–191, Wiley, Sussex, U.K.

Wu, J.-Y., C.-T. Lin, C. Brandon, T.-S. Chan, H. Möhler, and J. G. Richards (1982) Regulation and immunocytochemical characterization of glutamic acid decarboxylase. In *Cytochemical Methods in Neuroanatomy,* S. Palay and V. Chan-Palay, eds., pp. 279–296, Liss, New York.